Thermodynamic Linkage between Tubulin Self-Association and the Binding of Vinblastine†

George C. Na and Serge N. Timasheff*

ABSTRACT: A sedimentation velocity study has been carried out of the vinblastine-induced self-association of calf brain tubulin in PG (0.01 M NaP_i and 10^{-4} M GTP, pH 7.0) buffer as a function of vinblastine concentration and temperature. The dependence of the weight-average sedimentation coefficients ($\bar{s}_{20,w}$) on total protein concentration can be fitted best by an isodesmic, indefinite self-association mechanism. Apparent association constants, derived by computer fitting of the $\bar{s}_{20,w}$ data, were analyzed in terms of the Wyman linkage equations. Fitting to a variety of reaction models suggested that the self-association is one ligand molecule mediated; i.e., the binding of one vinblastine molecule is coupled to the formation of each intertubulin bond. The intrinsic association equilibrium constant for dimerization of the vinblastine-liganded tubulin was found to be 1.8×10^5 M^{-1}. The self-association is characterized by an apparent van't Hoff enthalpy change of +8.0 kcal/mol at 5×10^{-5} M vinblastine and is driven by a positive entropy change. Apparent binding isotherms of vinblastine to tubulin were calculated based on the association mechanism and parameters derived from the linkage analysis and were found to be consistent with the vinblastine binding results previously reported in our laboratory under identical conditions [Lee, J. C., Harrison, D., & Timasheff, S. N. (1975) *J. Biol. Chem. 250*, 9276–9282]. Comparison of apparent binding curves calculated with different values of the self-association constants suggested that cooperativity between ligand binding and self-association may account for the disparity of the vinblastine–tubulin binding constants reported in the literature.

In the preceding paper (Na & Timasheff, 1980) rigorous analysis of sedimentation velocity data on the self-association of tubulin induced by vinblastine has shown that this reaction can be described in terms of an indefinite isodesmic self-association model, in which tubulin subunits add to a growing chain with identical association constants for each step of the polymerization. The present paper is devoted to an analysis of the thermodynamics of the self-association process. Since this process is a consequence of interactions between tubulin and vinblastine, an understanding of the linkage between binding of the drug to tubulin and the polymerization reaction should help to elucidate not only the thermodynamic mechanistic aspects of this process but also the manner in which this antitumor agent and possibly other vinca alkaloids exercise their pharmacological action.

The interaction between vinblastine and tubulin has been the subject of a number of studies described in the literature. In an earlier examination of this problem, Owellen et al. (1972, 1974), using porcine and rat brain tubulins, reported that the number of vinblastine molecules bound to tubulin was approximately half of that of colchicine; i.e., the suggested binding stoichiometry was one vinblastine molecule per two tubulin dimers. More recent studies by Lee et al. (1975) using calf brain tubulin, by Wilson et al. (1975) using embryonic chick brain tubulin, and by Bhattacharyya & Wolff (1976) using rat brain tubulin have produced the consistent result that each tubulin dimer contains two vinblastine binding sites. The binding constants reported from these laboratories, however, differed greatly from each other. Lee et al. (1975) and Wilson et al. (1975) concluded that a tubulin dimer contains two equivalent binding sites, with a binding constant of $(2.2–2.4) \times 10^4$ M^{-1} (Lee et al., 1975) or $(3–5) \times 10^5$ M^{-1} (Wilson et al., 1975). On the other hand, Bhattacharyya & Wolff (1976) concluded that the two binding sites on rat brain tubulin are of different strengths, the binding constant of one site being 6.2×10^6 M^{-1} and that of the other site being 8×10^4 M^{-1}.

Compounding the strong disagreement about the value of the vinblastine binding constant, even less understanding exists of the molecular mechanism through which vinblastine inhibits microtubule formation, disrupts existing microtubules, and induces tubulin self-association. Wilson et al. (1975, 1976) have found that vinblastine, even when present at a level substoichiometric to tubulin, can inhibit the in vitro assembly of embryonic chick brain microtubules but cannot bind to or disrupt preformed sea urchin sperm tail outer doublet microtubules. They suggested that vinblastine may have a poisoning effect on microtubule assembly; i.e., the insertion of a tubulin dimer with vinblastine complexed to it during the assembly of a microtubule may stop its further growth. They also suggested that vinblastine binding sites on tubulin may be blocked when the protein is assembled into microtubules, preventing vinblastine from binding to or disrupting preformed microtubules. Using beef brain tubulin, Himes et al. (1976) have also found that a substoichiometric level of vinblastine is capable of inhibiting in vitro microtubule assembly. Furthermore, Bhattacharyya & Wolff (1976) reported that the values of the dissociation constants, of the "strong" and "weak" vinblastine binding sites, calculated from their data, appear to correspond to the concentrations of vinblastine needed for the in vitro inhibition of microtubule assembly and the induction of tubulin aggregation, respectively. From this correlation, they suggested that the vinblastine molecule bound to the strong binding site may inhibit microtubule assembly, whereas that bound to the weak binding site may induce the aggregation of tubulin.

While all of these studies neglected the linkage between the ligand binding and self-association reactions, it is evident that in the vinblastine-induced self-association of tubulin, the two reactions are obligatorily coupled to each other energetically. Therefore, the thermodynamic parameters reported in these

† From the Graduate Department of Biochemistry, Brandeis University, Waltham, Massachusetts 02254. *Received July 11, 1979.* Supported by grants from the National Institutes of Health (CA 16707 and GM 14603) and a National Research Service Award (CA 05538). This paper is Publication No. 1297.

0006-2960/80/0419-1355$01.00/0

studies (Lee et al., 1975; Wilson et al., 1975; Bhattacharyya & Wolff, 1976) must be regarded only as apparent values and any direct interpretation based on them can easily be erroneous and must be approached with great caution. Indeed, Cann & Hinman (1976) and Nichol & Winzor (1976) have shown that cooperativity between ligand binding and macromolecule self-association could result in ligand-binding curves resembling those characteristic either of cooperative binding between several ligand binding sites or of binding to several nonidentical sites. Proper analysis of the characteristic thermodynamic linkages between a ligand-binding reaction and a self-association reaction can be used to great advantage in obtaining rigorously valid information on the ligand-binding stoichiometry and the intrinsic association constants, as well as on the mechanism and thermodynamic parameters of the self-association. In this paper, we have analyzed the free-energy linkage between the vinblastine binding and the induced self-association of tubulin. This analysis has allowed us to deduce the vinblastine stoichiometry coupled to the self-association reaction and to assess the contributions of the "ligand-mediated" and "ligand-facilitated" pathways of the self-association. On the basis of the linkage analysis, a self-consistent explanation can be proposed for the diverse values reported in the literature for the tubulin–vinblastine binding constants. A preliminary report of these studies has been published (Na & Timasheff, 1979).

Materials and Methods

The method of calf brain tubulin preparation and the chemical reagents used were identical with those described in the preceding paper (Na & Timasheff, 1980). For the study of the temperature dependence of the self-association, tubulin was equilibrated with the experimental buffer at the desired temperature by using a jacketed Sephadex G-25 column connected to a heating and cooling circulating bath. In equilibrating tubulin with 1×10^{-5} M or lower concentrations of vinblastine, a precalculated amount of the drug was added to the protein before application to the column (1.7 × 25 cm) in order to avoid overdepletion of vinblastine from the gel. The velocity sedimentation experiments were then performed at the same temperature as that used in the gel column equilibration. Throughout this study, tubulin was always equilibrated with vinblastine in PG buffer[1] before use. Unless stated otherwise, the listed vinblastine concentrations denote the concentration of unbound vinblastine in the solution.

Results

As described in the preceding paper, in the presence of 2.5×10^{-5} M or higher concentrations of vinblastine in PG buffer, tubulin sediments in a single peak, skewed forward. As the concentration of free vinblastine is decreased, below 2.5×10^{-5} M, the boundary gradually resolves into a bimodal one due to the generation of a concentration gradient of free vinblastine across it. However, irrespective of protein and ligand concentration gradients in the reaction boundary, the movement of the second moment of the boundary always gives the weight-average sedimentation coefficient of the protein in the plateau region. The weight-average sedimentation coefficients of tubulin as a function of total protein concentration, for six different free vinblastine concentrations ranging from 1×10^{-6} to 5×10^{-4} M, are shown in Figure 1. At the higher concentrations of vinblastine, $\bar{s}_{20,w}$ increases hyperbolically with

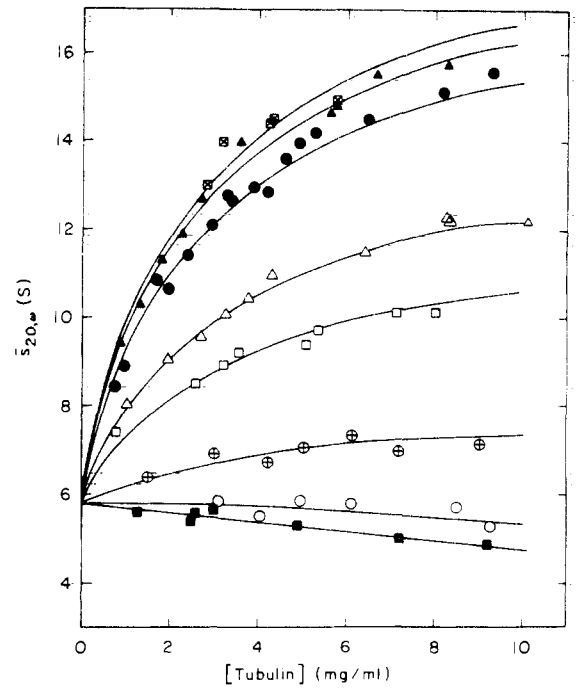

FIGURE 1: Weight-average sedimentation coefficients ($\bar{s}_{20,w}$) of tubulin determined as a function of total protein concentration. Tubulin was equilibrated with different concentrations of vinblastine [(■) PG only; (○) 1×10^{-6} M; (⊕) 5×10^{-6} M; (□) 2.5×10^{-5} M; (△) 5×10^{-5} M; (●) 1×10^{-4} M; (▲) 2×10^{-4} M; (⊠) 5×10^{-4} M] in PG buffer, using both a batch and a flow column of Sephadex G-25 gel as described under Materials and Methods; 0.5-mL aliquots were collected from the column and used directly for ultracentrifugation without dilution to avoid changes in free vinblastine concentration. The $\bar{s}_{20,w}$ values were obtained from numerical integration of the sedimentation boundaries as described in the preceding paper. Solid lines are least-squares fittings of the experimental data by the isodesmic, indefinite, self-association model described in the text.

Table I: Dependence of Tubulin Self-Association on Free Vinblastine Concentration

vinblastine concn (mol/L)	fitted K_2^{app} (L/mol)
5×10^{-4}	1.4×10^5
2×10^{-4}	1.3×10^5
1×10^{-4}	1.1×10^5
5×10^{-5}	5.4×10^4
2.5×10^{-5}	3.3×10^4
5×10^{-6}	8.8×10^3
1×10^{-6}	1.9×10^3

increasing tubulin concentration. At lower vinblastine concentrations, this trend gradually diminishes. At 1×10^{-6} M vinblastine, the lowest concentration studied, $\bar{s}_{20,w}$ actually decreased slightly with increasing tubulin concentration, indicating that the negative concentration dependence due to the hydrodynamic retardation overwhelmed the positive dependence due to self-association. The solid lines shown in Figure 1 are least-squares fittings of the data according to the isodesmic, indefinite self-association model described in the preceding paper (Na & Timasheff, 1980). It appears, therefore, that this reaction model can accommodate well the experimental data obtained over the entire vinblastine concentration range studied. Table I shows the apparent dimerization constants, K_2^{app}, obtained from curve fitting.

The equilibrium constant, K, for a macromolecular reaction in which reactants A and B form product C can be expressed as $K = [C]/[A][B]$, where [A], [B], and [C] are the molar concentrations of the reactants and product at chemical equilibrium. If the macromolecular reaction equilibrium is

[1] Abbreviation used: PG buffer, 0.01 M NaP_i and 1×10^{-4} M GTP, pH 7.0.

affected by a ligand X and the activities of all other ligands are held constant (Aune & Timasheff, 1971), the thermodynamic linkage between its equilibrium constant and interaction with ligand is given by (Wyman, 1964)

$$\left(\frac{\partial \ln K}{\partial \ln a_X}\right)_{T,P,a_{j\neq X}} = \left(\frac{\partial m_X}{\partial m_C}\right)_{T,P,m_{j\neq C}} - \left(\frac{\partial m_X}{\partial m_A}\right)_{T,P,m_{j\neq A}} - \left(\frac{\partial m_X}{\partial m_B}\right)_{T,P,m_{j\neq B}} \quad (1)$$

where a_X is the thermodynamic activity of the ligand X and $(\partial m_X/\partial m_i)_{T,P,a_{j\neq i}}$ is the preferential binding of ligand X to species i of the macromolecule. The preferential binding term is, in fact, a sum of the total ligand binding and the total hydration (Tanford, 1969; Inoue & Timasheff, 1972; Lee & Timasheff, 1977)

$$\left(\frac{\partial \ln K}{\partial \ln a_X}\right)_{T,P,a_{j\neq X}} = (\bar{X}_C - \bar{X}_A - \bar{X}_B) - \frac{[X]}{[W]}(\bar{W}_C - \bar{W}_A - \bar{W}_B) \quad (2)$$

where [W] is the molar concentration of water in the solution, [X] is that of free ligand; $\bar{W}_i$ is the total hydration of the macromolecular species i, and $\bar{X}_i$ is the total ligand binding by the macromolecular species i. If a ligand interacts strongly with the macromolecule, the effect of the ligand on the macromolecular reaction manifests itself at a concentration where $[X] \ll [W]$, which permits us to neglect the second term in eq 2 and also to use [X] in the place of a_X since the activity coefficient of the ligand should be essentially equal to 1.0.

In defining the reaction equilibrium constant, K, the concentration terms [A], [B], and [C] represent the total concentrations of the corresponding species without distinction between molecules with different extents of binding of the various ligands (Wyman, 1964). This equilibrium constant is, therefore, an apparent quantity. In the case of self-association reactions, it is identical with those determined by the usual physical techniques such as sedimentation, light scattering, or gel filtration, which measure macromolecular properties and are usually insensitive to the extent of interaction of the macromolecule with low molecular weight ligands.

In eq 2, $\bar{X}_i$ is defined as the average number of moles of the ligand X bound per mole of macromolecule i. $\Delta\bar{X} = \bar{X}_C - \bar{X}_A - \bar{X}_B$ is then the difference of such average ligand binding between the product and the reactants, and $\Delta\bar{X}$ should have a value between zero and the ligand stoichiometry in the macromolecular reaction, i.e., the number of ligand molecules bound or dissociated during the course of the reaction. An analysis, therefore, of $(\partial \ln K/\partial \ln a_X)_{T,P,a_{j\neq X}}$ or $\Delta\bar{X}$ as a function of the ligand concentration should lead to the ligand stoichiometry in the reaction. Furthermore, a detailed study of $\Delta\bar{X}$ as a function of ligand concentration can shed some light on the relative probability of various reaction pathways. Let us illustrate this by using, as an example, a simple macromolecular dimerization which can proceed through either a ligand-mediated or a ligand-facilitated pathway, as described below.

(1) Ligand-mediated dimerization reaction. A ligand-mediated reaction has been defined as one in which ligand binding must precede the macromolecular reaction (Tai & Kegeles, 1975; Kegeles & Cann, 1978). For the dimerization involving one ligand molecule per protein monomer, we may express the reactions by pathway I of eq 3:

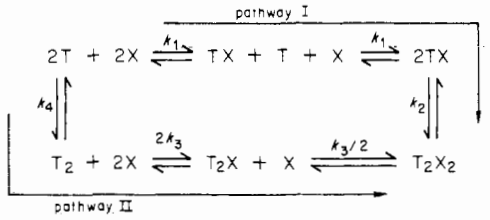

(3)

T denotes the macromonomer and X the ligand; k_1 and k_2 are the equilibrium constants for the ligand-binding and the dimerization reactions, respectively. In this pathway, the binding of the ligand molecule X induces a change in the macromolecule, e.g., in the charge distribution or conformation, which renders it capable of polymerization. For the mechanism written in this way, the monomers will not be able to self-associate without first binding the ligand. The dimers, on the other hand, bind the ligand X strongly and do not release it without first dissociating into monomers. The apparent self-association constant, K_2^{app}, and the Wyman function (eq 2) for such a dimerization reaction can be expressed as

$$K_2^{app} = \frac{[(TX)_2]}{([T] + [TX])^2} = \frac{k_2}{[1 + 1/(k_1[X])]^2} \quad (4)$$

and

$$\left(\frac{\partial \ln K_2^{app}}{\partial \ln [X]}\right)_{T,P,a_{j\neq X}} = \Delta\bar{X} = \left(\frac{\partial \ln k_2}{\partial \ln [X]}\right)_{T,P,a_{j\neq X}} + \frac{2}{1 + k_1[X]} = \frac{2}{1 + k_1[X]} \quad (5)$$

since k_2 is the dimerization constant of the liganded macromonomers and is independent of [X]. The solid lines in parts A and B of Figure 2 are plots of $\ln K_2^{app}$ and $\Delta\bar{X}$ as a function of ln [X]. For the ligand-mediated dimerization, $\ln K_2^{app}$ increases with increasing [X]; the curve displays a downward curvature at high values of [X]. $\Delta\bar{X}$, on the other hand, follows a sigmoidal dependence on ln [X]; at very high ligand concentrations it approaches zero asymptotically. As [X] decreases, its value increases, reaching 1.0 at $k_1[X] = 1$, and then approaches 2.0, the ligand stoichiometry of the dimerization reaction, at an infinitely low concentration of the ligand.

(2) A ligand-induced dimerization reaction with an overall identical stoichiometry can also proceed through an alternate mechanism totally different from the one shown above, namely, through a ligand-facilitated pathway, i.e., one in which ligand binding follows the macromolecular reaction and stabilizes the products (Kegeles & Cann, 1978). For dimerization, this is shown by pathway II of eq 3. In this mechanism, although the self-association reaction is also driven by the binding of one ligand per macromonomer, the macromonomer can self-associate into dimers even without binding the ligand. Contrary to the ligand-mediated association, the ligand can bind only to the dimers and not to the monomers; the self-association generates a binding site. The liganded macrodimers are stable with respect to dissociation and will not dissociate into monomers without first releasing the bound ligands. The apparent self-association constant for this mechanism can be expressed as

$$K_2^{app} = \frac{[T_2] + [T_2X] + [T_2X_2]}{[T]^2} = k_4(1 + 2k_3[X] + k_3^2[X]^2) \quad (6)$$

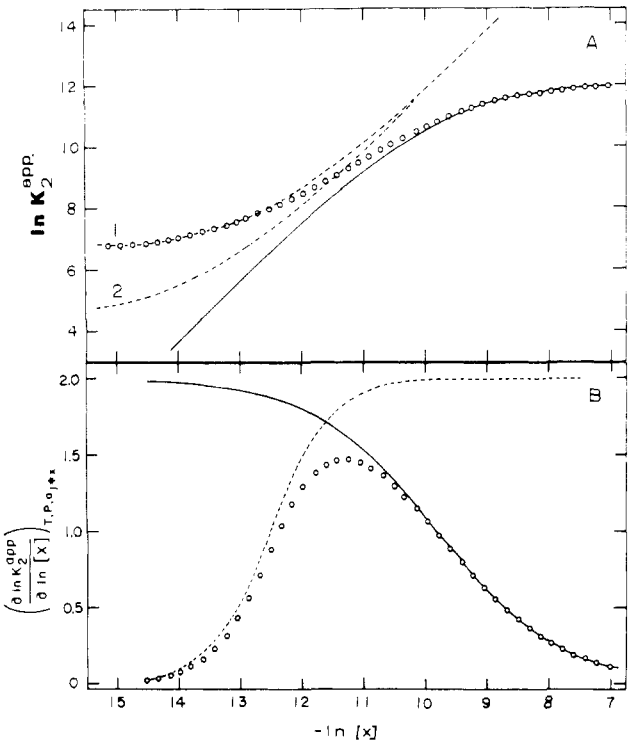

FIGURE 2: Wyman plots of the apparent dimerization constant for the ligand-mediated, ligand-facilitated, and ligand-mediated plus -facilitated mechanisms of self-association. (A) ln K_2^{app} vs. ln [X]. The solid line is for ligand-mediated self-association, where $k_1 = 1.8 \times 10^4$ M^{-1} and $k_2 = 1.8 \times 10^5$ M^{-1}. The two dashed lines are for ligand-facilitated self-association where the intrinsic equilibrium constants used are (1) $k_3 = 2.7 \times 10^5$ M^{-1} and $k_4 = 8 \times 10^2$ M^{-1} and (2) $k_3 = 8.5 \times 10^5$ M^{-1} and $k_4 = 80$ M^{-1}. The open circles are for the ligand-mediated plus -facilitated mechanism of self-association where $k_1 = 1.8 \times 10^4$ M^{-1}, $k_2 = 1.8 \times 10^5$ M^{-1}, $k_3 = 2.7 \times 10^5$ M^{-1}, and $k_4 = 8 \times 10^2$ M^{-1}. (B) $(\partial \ln K_2^{app}/\partial \ln [X])_{T,P,a_{j\neq X}}$ vs. ln [X]; the symbols have the same meaning as in (A).

Since k_4 is the dimerization constant of the unliganded macromonomers, it is independent of [X] and

$$\left(\frac{\partial \ln K_2^{app}}{\partial \ln [X]}\right)_{T,P,a_{j\neq X}} = \Delta\bar{X} = \frac{2k_3[X] + 2k_3^2[X]^2}{1 + 2k_3[X] + k_3^2[X]^2} \quad (7)$$

The dashed lines in parts A and B of Figure 2 are plots of ln K_2^{app} and $\Delta\bar{X}$ as a function of ln [X] for the ligand-facilitated dimerization. It is evident that the K_2^{app} values for the ligand-mediated and ligand-facilitated association mechanisms are different functions of ln [X]. For the ligand-facilitated dimerization, the plot of ln K_2^{app} vs. ln [X] displays an upward curvature; $\Delta\bar{X}$ has a value of zero at infinitely low ligand concentration, reaches 1.0 at $k_3[X] = 1$, and approaches 2.0, namely, the ligand stoichiometry in the self-association reaction, at infinitely high ligand concentration.

(3) Combined ligand-mediated and -facilitated dimerization reaction. While the preceding distinction will be true if one of the pathways is kinetically blocked relative to the duration of the experiment, it is certainly possible that both described pathways of eq 3 are kinetically permitted and maintain equilibrium during the time course of the measurements. In this case, the apparent dimerization constant and the Wyman function can be expressed as

$$K_2^{app} = \frac{[T_2] + [T_2X] + [T_2X_2]}{([T] + [TX])^2} = k_4\frac{1 + 2k_3[X] + k_3^2[X]^2}{(1 + k_1[X])^2} \quad (8)$$

and

$$\left(\frac{\partial \ln K_2^{app}}{\partial \ln [X]}\right)_{T,P,a_{j\neq X}} = \Delta\bar{X} = \frac{2k_3[X] + 2k_3^2[X]^2}{1 + 2k_3[X] + k_3^2[X]^2} - \frac{2k_1[X]}{1 + k_1[X]} \quad (9)$$

These equations are plotted in parts A and B of Figure 2 by the open circles. For the combined ligand-mediated and -facilitated mechanism of self-association, the apparent association constant approaches that of the mediated mechanism at high ligand concentration and that of the facilitated mechanism at low ligand concentration. For the derivative plot, $\Delta\bar{X}$ approaches zero at both the high and low ligand concentration ends, while between these two extremes it reaches a maximal value which is a function of the two ligand binding constants, k_1 and k_3, and is less than the ligand stoichiometry in the dimerization reaction.

The examples developed above indicate that in a Wyman-type plot, the slope is never equal to the exact stoichiometry of the number of ligand molecules involved in a reaction. In fact, this slope is a lower limit to the stoichiometry and may be significantly different from it. Equations 5, 7, and 9, which were developed specifically for the treatment of the vinblastine-dependent self-association of tubulin, are, in fact, particular cases of more general expressions for ligand-induced self-association. Let us consider a reaction with a degree of self-association r and involving a number of ligand molecules per monomer $\Delta\nu$ bound at independent equivalent multiple sites, all equally linked to the association. For this case, the linkage expression for the combined ligand-mediated and ligand-facilitated reaction can be written out as, properly taking statistical factors into account (Klotz, 1953)

$$\left(\frac{\partial \ln K^{app}}{\partial \ln [X]}\right)_{T,P,a_{j\neq X}} = r\Delta\nu - \frac{\sum_{i=1}^{n} i\frac{n!}{[(n-i)!](i!)}k_3^{n-i}[X]^{n-i}}{1 + \sum_{i=1}^{n}\frac{n!}{[(n-i)!](i!)}k_3^{i}[X]^{i}} - r\frac{\sum_{i=1}^{n} i\frac{n!}{[(n-i)!](i!)}k_1^{i}[X]^{i}}{1 + \sum_{i=1}^{n}\frac{n!}{[(n-i)!](i!)}k_1^{i}[X]^{i}} \quad (10)$$

where i is the number of ligand molecules bound to any species and $n = r\Delta\nu$. The corresponding expressions for the independent ligand-mediated and ligand-facilitated pathways are obtained from eq 10 by eliminating the second or the third term on the right-hand side, respectively. It is evident that in each case, the slope of the ln K vs. ln [X] plot is always less than $r\Delta\nu$. It can approach $r\Delta\nu$ for the independent pathways only at extremes of ligand concentration.

Analysis of the Linkage between Vinblastine Binding and Tubulin Self-Association. The data of Figure 1 and Table I were analyzed in terms of the linkage functions described in the previous section in order to elucidate the exact stoichiometry and the linkage mechanism between the vinblastine binding and the tubulin self-association. A plot of ln K_2^{app} as a function of ln [X] shown in Figure 3A indicates that the equilibrium constant increases with increasing ln [X]. The slope between each two consecutive points decreases gradually with increasing ln [X], from 0.95 between 1×10^{-6} and 5×10^{-6} M vinblastine to 0.07 between 2×10^{-4} and 5×10^{-4} M vinblastine. The gradual attainment of a plateau in the de-

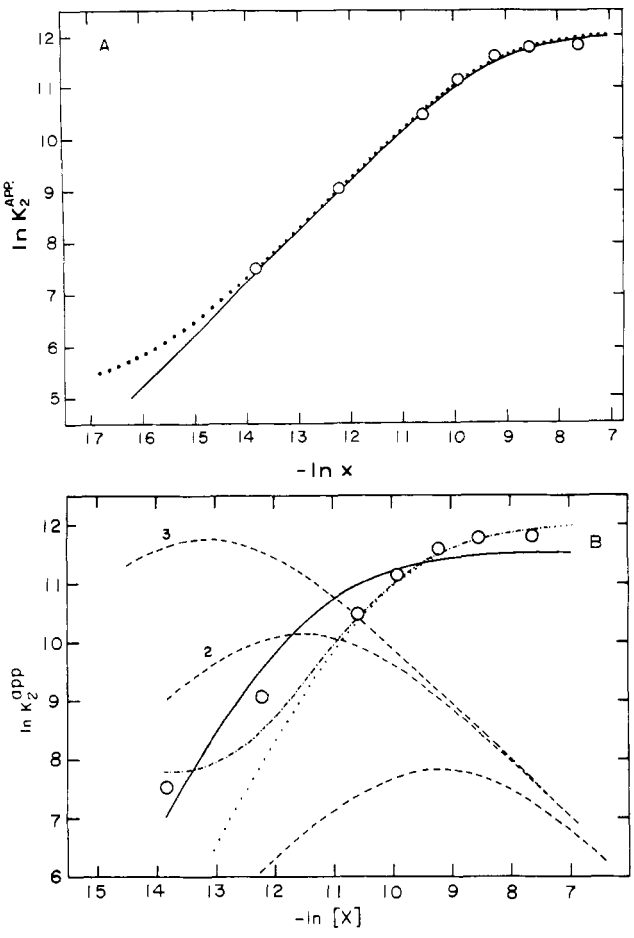

FIGURE 3: Wyman plot of the experimental apparent dimerization constants for the vinblastine-induced self-association of tubulin and their least-squares fittings by different reaction mechanisms. The experimental results are depicted by the open circles. (A) Least-squares fittings by mechanisms 1a (—) and 1c (···). (B) Least-squares fittings by mechanism 2a at [vinblastine] $\geq 1 \times 10^{-6}$ M (—) and at [vinblastine] $\geq 2.5 \times 10^{-5}$ M (···) and mechanism 2b (-·-). The intrinsic equilibrium constants derived from these fittings, together with the sum of the squares of the deviation, are shown in Table II. The dashed lines in (B) are the Wyman plots for self-association via a cross-linking mechanism as described by eq 15 and 16 in the text. The intrinsic equilibrium constants, k_1, used in this case are (1) 1×10^4, (2) 1×10^5, and (3) 5×10^5 M^{-1}.

pendence of the apparent association constants on free vinblastine concentration indicates that the ligand-mediated pathway is kinetically open and probably predominates in this process, although the ligand-facilitated mechanism cannot be fully excluded. As a result, in fitting the experimental data, we used only the ligand-mediated and the combined mediated plus facilitated mechanisms of association. Since each tubulin dimer has two vinblastine binding sites, it is possible that the self-association is linked to the binding of either one or two vinblastine molecules. Let us consider these in turn.

(1) Vinblastine Stoichiometry = 1. This mechanism requires the binding of one vinblastine molecule for the formation (ligand-mediated mechanism) or stabilization (ligand-facilitated mechanism) of each intertubulin bond. (1a) In this variation of the mechanism, only one vinblastine binding site is pertinent to the self-association; i.e., the binding of vinblastine to the second site is unaffected by the self-association state of the macromolecule and its binding constant remains equal to that of the monomer. For this stoichiometry, assuming a ligand-mediated pathway and taking account of the possible ways of forming any given bond through introduction of proper statistical factors, the reaction equilibria, the apparent association constant, and the linkage can be expressed by pathway I of eq 11:

Table II: Least-Squares Fitting of the Linkage by Different Reaction Models

mechanism	k_1 (L/mol)	k_2 (L/mol)	k_3 (L/mol)	k_4 (L/mol)	SSD[a]
1a	1.8×10^4	1.8×10^5			0.06
1b	9.0×10^3	1.8×10^5			0.06
1c	1.8×10^4	1.8×10^5	1.0×10^7	1.6×10^2	0.06
2a	3.1×10^4	1.7×10^5			0.05[b]
	6.1×10^4	1.3×10^5			0.28[c]
	9.0×10^4	1.2×10^5			1.22[d]
2b	3.1×10^4	1.7×10^5	2.6×10^5	2.4×10^3	0.46

[a] Sum of square of deviation. [b] Fitted with data where [vinblastine] $\geq 2.5 \times 10^{-5}$ M. [c] Fitted with data where [vinblastine] $\geq 5.0 \times 10^{-6}$ M. [d] Fitted with data where [vinblastine] $\geq 1.0 \times 10^{-6}$ M.

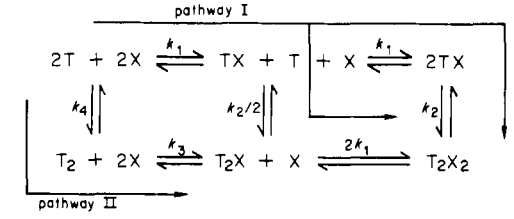

(11)

$$K_2^{app} = \frac{[T_2X] + [T_2X_2]}{([T] + [TX])^2} = \frac{k_1k_2[X](1 + 2k_1[X])}{2(1 + k_1[X])^2} \quad (12)$$

$$\left(\frac{\partial \ln K_2^{app}}{\partial \ln [X]}\right)_{T,P,a_{j\neq X}} = \frac{1 + 3k_1[X]}{(1 + k_1[X])(1 + 2k_1[X])} \quad (13)$$

The least-squares fitting by the above mechanism of the apparent association constants from Table I is shown by the solid line in Figure 3A. It is evident that the calculated curve fits the data quite well over the entire range of vinblastine concentration. The intrinsic reaction equilibrium constants derived from this fitting, together with the sum of the squares of deviations found, are listed in Table II under mechanism 1a.

(1b) A second variation of this mechanism is one in which the two vinblastine binding sites on each tubulin dimer are equivalent. The binding of one vinblastine molecule to any one of the two sites enables the protein to self-associate; i.e., the binding of the second vinblastine molecule to a tubulin dimer does not enhance any further the intrinsic self-association constant of the protein. This mechanism results in a linkage relation identical with that of mechanism 1a (eq 13), except that the intrinsic ligand binding constant, k_1, will have a value equal to one-half of that found in mechanism 1a due to the doubling of the number of ligand binding sites that can induce self-association and the resulting statistical factor in the equilibrium relation (eq 12).

(1c) For the combined mediated plus facilitated mechanism of self-association, both paths of eq 11 must be considered. Since $k_1k_2 = 2k_3k_4$, the apparent association constant becomes

$$K_2^{app} = \frac{[T_2] + [T_2X] + [T_2X_2]}{([T] + [TX])^2} = k_4\frac{1 + k_3[X](1 + 2k_1[X])}{(1 + k_1[X])^2} = \frac{k_1k_2[X](1 + 2k_1[X])}{2(1 + k_1[X])^2} + \frac{k_4}{(1 + k_1[X])^2} \quad (14)$$

where the first term is identical with the apparent association constant shown in eq 12. The data of Figure 1 and Table I were fitted to the above equation, and the results are shown

by the dotted line in Figure 3A. This curve was obtained by using the same values of k_1 and k_2 as for the solid line but varying the value of k_4. It is evident that the right-hand half of the curve which is determined largely by the equilibrium constants k_1 and k_2 is essentially identical with that predicted by the ligand-mediated mechanism. Introducing the facilitated pathway only lifts the left-hand portion of the curve until it levels off gradually at ln k_4, instead of decreasing continuously with decreasing ligand concentration. This effect is evident from eq 14, where the second term becomes significant only for $[X] \ll k_1^{-1}$. The results of these fittings show that the ligand-facilitated pathway of tubulin self-association cannot be ruled out, although the value of k_4 cannot be greater than 1.9×10^3 M^{-1}, above which significant deviations from the data appear.

(2) *Vinblastine Stoichiometry = 2.* The reaction mechanisms for this stoichiometry have been described above in the general discussion of linkage. For the ligand-mediated pathway, described by eq 4 and 5, the solid line in Figure 3B represents its least-squares fitting to the experimental data. This mechanism does not lead to a good fitting of the experimental points, since it predicts a slope of 2 at low ligand concentration, whereas the experimental data approach a slope of 1. Since the apparent association constant obtained at higher vinblastine concentrations has a smaller relative experimental error, these points should be given greater weight. However, a fitting to these points alone, shown by the dotted line of Figure 3B, resulted in good agreement only with the points at higher vinblastine concentrations but in substantial deviations from experimental data at low ligand concentrations. Use of the ligand-mediated plus -facilitated mechanism, described by eq 8 and 9, lifts up the left-hand portion of the Wyman plot, resulting in the much better fit shown by the dot–dash line of Figure 3B and the parameters listed in Table II under mechanism 2B.

(3) *Cross-Linking Mechanism of Self-Association.* In this self-association mechanism, the vinblastine molecules serve essentially as cross-linkers between two tubulin dimers by binding to both protein molecules. On the assumption that all the ligand–macrmolecule interactions are equivalent with an association constant equal to k_1, the reactions, equilibrium constants, and linkage can be expressed as

$$T + X \overset{k_1}{\rightleftharpoons} TX$$

$$TX + T \overset{k_1}{\rightleftharpoons} TXT$$

$$TX + X \overset{k_1}{\rightleftharpoons} XTX$$

$$XTX + T \overset{k_1}{\rightleftharpoons} XTXT$$

$$XTXT + X \overset{k_1}{\rightleftharpoons} XTXTX \qquad (15)$$

$$K_2^{app} = \frac{[T_2X] + [T_2X_2] + [T_2X_3]}{([T] + [TX] + [TX_2])^2} = \frac{k_1^2[X]}{(1 + k_1[X])^2} \qquad (16)$$

$$\left(\frac{\partial \ln K_2^{app}}{\partial \ln [X]}\right)_{T,P,a_{j\neq X}} = \frac{1 - k_1[X]}{1 + k_1[X]} \qquad (17)$$

This mechanism predicts a decrease of the apparent association constant at ligand concentrations $[X] > 1/k_1$. The experimental values of K_2^{app}, however, are still increasing at (2–5) $\times 10^{-4}$ M vinblastine, essentially eliminating this mechanism. This fit is well demonstrated by the three dashed lines of Figure 3B, calculated for k_1 values of 1×10^4, 1×10^5, and 5×10^5 M^{-1}.

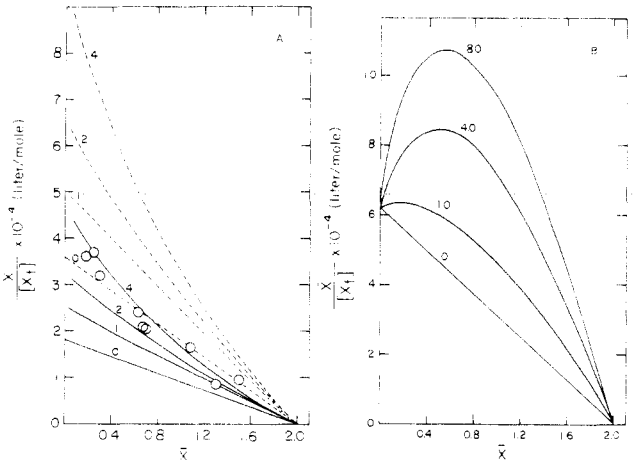

FIGURE 4: Calculated Scatchard plots of ligand binding coupled to protein self-association according to various association mechanisms and using the least-squares fitted intrinsic equilibrium constants found in the tubulin–vinblastine system. (A) Linked binding site = 1; unlinked binding site = 1. The dashed lines were calculated for mechanism 1a with $k_1 = 1.8 \times 10^4$ M^{-1} and $k_2 = 1.8 \times 10^5$ M^{-1}. The total protein concentrations are 0, 1.0, 2.0, and 4.0 mg/mL, as marked on the figure. The solid lines were calculated for mechanism 1b where $k_1 = 9 \times 10^3$ M^{-1}, $k_2 = 1.8 \times 10^5$ M^{-1}, and the protein concentrations are 0, 1.0, 2.0, and 4.0 mg/mL. The binding data of vinblastine to tubulin, reported by Lee et al. (1975), are shown by the open circles. (B) Linked ligand binding sites = 2. Calculated according to the linkage equation of mechanism 2a with $k_1 = 3.1 \times 10^4$ M^{-1} and $k_2 = 1.7 \times 10^5$ M^{-1}. The total protein concentrations are 0, 1.0, 4.0, and 8.0 mg/mL, as marked on the figure. For a more detailed description of the mechanism and calculations, see the text.

Calculation of the Apparent Binding Curves of Vinblastine. The binding isotherms of vinblastine to tubulin predicted by the different pathways described above were calculated for an isodesmic, indefinite ligand-mediated self-association in order to differentiate further between the various self-association mechanisms. They are presented in parts A and B of Figure 4 in the format of "Scatchard plots" (Scatchard, 1949).

For an association reaction described by a particular linkage relation and a given free ligand concentration, the concentration of the monomer and all polymeric species at any total protein concentration can be calculated from the intrinsic association constants of Table II by using eq 3–6 of the preceding paper (Na & Timasheff, 1980). On the assumption of a ligand-mediated association mechanism, all tubulin molecules in the polymeric species will have their linked vinblastine binding sites occupied. Binding of the vinblastine to those sites not linked to the self-association should be equivalent to vinblastine binding to dimers and can be calculated by using the intrinsic binding constant. Figure 4A displays the calculated binding isotherms for different total protein concentrations for a vinblastine stoichiometry of 1 in the self-association, according to mechanisms 1a and 1b. The resulting curves are presented by the solid and dashed lines, respectively. Equation 12 was used for calculating K_2^{app}, and the concentration of bound ligand was calculated from

$$[X_{bound}] = \sum_{i=1}^{\infty} \frac{C_i(i-1)}{iM} + \sum_{i=1}^{\infty} \frac{C_i}{iM} \frac{k_1[X_f]}{1 + k_1[X_f]} + \frac{C_{total}}{M} \frac{k_1[X_f]}{1 + k_1[X_f]} \qquad (18)$$

where C_i is the weight concentration of the ith polymer, M is the molecular weight of the tubulin dimer, C_{total} is the total protein weight concentration, k_1 is the intrinsic ligand binding constant to tubulin dimers, and $[X_f]$ is the concentration of free ligand. In this equation, the first term on the right-hand

Table III: Temperature Dependence and Thermodynamic Parameters of the Vinblastine-Induced Tubulin Self-Association in PG, pH 7.0[a]

temp (K)	fitted K_2^{app} (L/mol)
283.16	3.5×10^4
293.16	5.4×10^4
298.16	6.4×10^4
303.16	9.1×10^4

$\Delta G^\circ = -7.0$ kcal/mol at 20 °C
$\Delta H^{app} = +8.0$ kcal/mol at [vinblastine] = 5×10^{-5} M
$\Delta H^\circ = +4.0$ kcal/mol[b]
$\Delta S^\circ = +38$ eu

[a] Studied at a constant vinblastine concentration of 5×10^{-5} M. [b] Calculated according to eq 20.

side represents the binding to sites involved in self-association within polymers, the second term takes into account terminal sites on oligomers from monomer through all polymers, and the third term corresponds to the liganding of the self-association independent site. At finite protein concentrations, the resulting binding curves show a slight upward curvature, which increases with increasing total protein concentration.

The binding isotherms for a vinblastine stoichiometry of 2 in the self-association of tubulin are shown in Figure 4B. By use of the intrinsic association constants of mechanism 2a in Table II, the apparent association constants were calculated according to eq 4. The concentration of bound ligand was obtained according to

$$[X_{bound}] = \sum_{i=1}^{\infty} \frac{2C_i(i-1)}{iM} + \sum_{i=1}^{\infty} \frac{2C_i}{iM} \frac{k_1[X_f]}{1 + k_1[X_f]} \quad (19)$$

The two terms on the right-hand side of the equation correspond respectively to the binding of ligand to sites involved in polymerization and the terminal sites on all species. The resulting apparent binding curves at a finite protein concentration depart even more drastically from the intrinsic one than when the stoichiometry is 1. In fact, they pass through a maximum near $\bar{X} = 0.5$, falling back toward the intrinsic binding isotherm as free ligand decreases further.

The data on the binding of vinblastine to tubulin previously reported from our laboratory (Lee et al., 1975) under identical conditions with the present studies, except that the temperature was 25 °C instead of 20 °C, are shown by the open circles of Figure 4A. They seem to fit best the calculated curve for mechanism 1b, although the scatter of points makes it difficult to exclude mechanism 1a. On the other hand, these points certainly do not conform to the self-association mechanism involving two vinblastine molecules per tubulin–tubulin contact, permitting the elimination of that mechanism from consideration.

Temperature Dependence of the Self-Association. The dependence of the vinblastine-induced self-association of tubulin on solution temperature was studied from 10 to 30 °C. Tubulin was equilibrated with 5×10^{-5} M vinblastine in PG buffer at the desired temperature. The protein was then centrifuged at the same temperature and its weight-average sedimentation coefficient determined through numerical integration as described in the preceding paper. The data were corrected to obtain $\bar{s}_{20,w}$. Figure 5 shows the dependence of $\bar{s}_{20,w}$ on the total protein concentration at 10, 20, 25, and 30 °C. Again, at all four temperatures studied, the experimental data appear to be well fitted by the $\bar{s}_{20,w}$ curve calculated for the isodesmic, indefinite self-association model, as shown by the solid lines in the same figure. Table III presents the apparent dimerization constants at these temperatures obtained through the above curve fitting. The self-association is enhanced by an increase in temperature. A van't Hoff plot of the data is shown in the inset of Figure 5. A linear least-squares fitting of the points gave an apparent standard enthalpy change of +8.0 kcal/mol for the association reaction in the presence of 5×10^{-5} M free vinblastine.

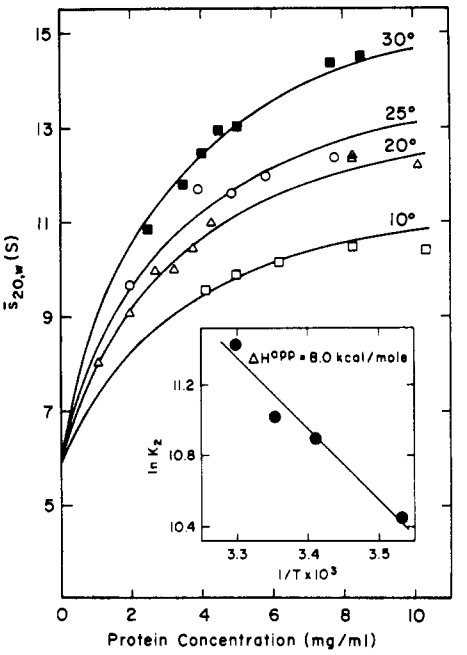

FIGURE 5: Weight-average sedimentation coefficients of tubulin as a function of temperature. Tubulin samples were equilibrated with 5×10^{-5} M vinblastine–PG buffer at constant temperature as described under Materials and Methods; 0.5-mL aliquots were collected from the Sephadex G-25 column and centrifuged at the same temperature as used in equilibrating the protein. The weight-average sedimentation coefficients obtained were corrected to obtain $\bar{s}_{20,w}$. Solid lines represent least-squares fitting of the experimental data by the isodesmic, indefinite self-association model. The temperatures are (□) 10, (△) 20, (○) 25, and (■) 30 °C. The inset is the van't Hoff plot of the apparent self-association constants obtained from the above fittings.

By adoption of the mechanism for the vinblastine-induced tubulin self-association described by eq 12, the apparent enthalpy change is

$$\Delta H_2^{app} = \left[\frac{\partial \ln K_2^{app}}{\partial(1/T)}\right]_{P,a_j} = \Delta H^\circ_2 + \Delta H^\circ_1 \frac{1 + 3k_1[X]}{(1 + k_1[X])(1 + 2k_1[X])} \quad (20)$$

where ΔH°_1 and ΔH°_2 are the van't Hoff standard enthalpy changes for the ligand-binding and the self-association reactions, respectively. In calculating ΔH°_2 with eq 20, ΔH°_1 can be approximated by 5.8 kcal/mol (Lee et al., 1975). This value was determined at a tubulin concentration of less than 0.6 mg/mL, where the degree of self-association is low and its contribution should be small. Setting the free ligand concentration, [X], equal to 5×10^{-5} M in eq 20, ΔH°_2 is found to be +4.0 kcal/mol. The temperature dependence of the self-association and the derived thermodynamic parameters are summarized in Table III, which shows that the self-association is driven by a positive entropy change of 38 eu, suggesting that hydrophobic and/or electrostatic forces are involved in the intertubulin interactions (Timasheff, 1973).

Discussion

The results described above demonstrate clearly the linkage between vinblastine binding and tubulin self-association. Analysis of the sedimentation velocity patterns as a function

of both protein and ligand concentration has permitted us to gain some insight into the mechanism and stoichiometry of the self-association. The linkage function, however, is mechanism dependent as shown by the analysis of two simple reaction pathways, namely, the ligand-mediated and ligand-facilitated self-associations.

The ligand-mediated and ligand-facilitated mechanisms of macromolecular self-association are usually not easy to distinguish. Knowledge that the self-association can proceed in the absence of the ligand but that it is enhanced by addition of the ligand is a good indication that the ligand-facilitated mechanism of self-association is operative. On the other hand, the inability to demonstrate self-association in the absence of the ligand does not necessarily exclude this mechanism, since the association equilibrium could be so weak in the absence of the ligand as to be undetectable by the available techniques. Although the three reaction paths shown in parts A and B of Figure 2 do exhibit different functional linkages of their apparent association constants with the ligand activity, such fits cannot be used to differentiate between them unequivocally, since accurate association constants can be obtained over only a very limited concentration range. Thus, while a monotone increase in the apparent association constant with increasing ligand activity suggests a ligand-facilitated mechanism and a similar monotone decrease in the apparent association constant with decreasing ligand activity suggests a ligand-mediated mechanism, with no apparent tendency of leveling off in either case, it is not possible to exclude the parallel existence of a strong ligand-mediated association in the first case and of a weak ligand-facilitated association in the second case.

In the vinblastine-induced self-association of tubulin, the apparent association constant reaches a plateau at high vinblastine concentration but decreases continuously at low ligand concentrations. These results definitely establish the operation of a ligand-mediated mechanism but cannot exclude the simultaneous participation of the ligand-facilitated pathway, with extremely weak self-association in the absence of the ligand and very strong binding of the ligand to polymerized tubulin. Since for the overall reaction the net free energy change between the reactants and product is independent of the reaction mechanism, the final selection of the reaction pathway must depend on the kinetics of the reaction. If the reaction rate through one pathway is very slow relative to the length of the experiment, its intermediates would never accumulate in any significant amount and it would have the appearance of being closed. Tai & Kegeles (1975) have used such kinetic studies to demonstrate that the Ca^{2+}-induced hexamer–dodecamer association of lobster hemocyanin proceeds through a ligand-mediated and not a ligand-facilitated or mediated plus facilitated mechanism. In the present paper, we have demonstrated that analysis in terms of thermodynamic linkage can be used to eliminate some reaction mechanisms. It should be emphasized, however, that just as in any other mechanistic study, the number of the mechanisms that can be proposed is essentially unlimited. Comparison of experimental data with theoretical curves calculated on the basis of various proposed mechanisms can be used only to eliminate a mechanism but will never result in unequivocal proof that a given mechanism is the correct one for the system under examination. However, while a true equilibrium constant, i.e., the equilibrium constant between two thermodynamically defined states, is totally independent of the reaction pathway, an apparent equilibrium constant, which for a self-association reaction is simply the ratio of the total concentration of the associated species to the total concentration of the unassociated species, without any regard for any other linked reactions, will be a function of the pathway of the reaction and, thus, can be used as a test of the validity of various mechanisms.

The slope of the Wyman plot shown in Figure 3 suggests a stoichiometry of one vinblastine molecule bound to tubulin during the formation of each intertubulin bond. Actual data fittings, listed in Table II, however, show that a ligand stoichiometry of 2, in a combined mediated plus facilitated mechanism, also fits the data reasonably well. In the region of low ligand activity, a definite divergence appears between the linkages which correspond to these two stoichiometries, with the data favoring the one vinblastine molecule coupling. This difference, however, becomes significant only under conditions where the tubulin self-association is very weak and the experimental errors are large, rendering any unequivocal choice perilous. It would appear more cautious, therefore, to take the slope of the Wyman plot only as a lower limit for the stoichiometry of the ligand binding which accompanies the self-association of the protein.

An alternate and complementary way of looking at ligand stoichiometry is afforded by an examination of the ligand binding under different association conditions. This approach has the advantages that accurate binding data can be obtained over a wide ligand concentration range and that measurements of ligand binding do not involve any assumptions concerning macromolecule hydrodynamic properties as is required in deducing an apparent association constant in a polymerization reaction through velocity sedimentation studies. The choice between stoichiometries, however, still requires comparison with theoretical curves calculated for the various cases. Such theoretical curves have been calculated for mechanisms 1a, 1b, and 2a of Table II, and they are shown in parts A and B of Figure 4 in the form of Scatchard plots. It is evident that stoichiometries of one and two ligand molecules bound per addition of tubulin dimer to the growing polymer result in binding curves with drastically different characters, as has been shown previously by Cann & Hinman (1976). Linkage of protein self-association with the binding of two ligand molecules leads to a maximum in the Scatchard plot at $\bar{X} \simeq 0.5$. Since such a maximum was not observed in the binding data reported previously from this laboratory (Lee et al., 1975) (see Figure 4A), the stoichiometry of 2 can be reasonably rejected and it seems most likely that the tubulin self-association is induced by the binding of one vinblastine molecule per dimer. In this regard, it is interesting to note that the paracrystalline aggregates of tubulin induced by vinblastine in vivo contain approximately one vinblastine molecule bound per tubulin dimer (Bryan, 1972). This result has been confirmed by Wilson et al. (1978), who have demonstrated furthermore that the isolated tubulin paracrystalline aggregates, if incubated with vinblastine in vitro, can bind one vinblastine molecule per tubulin dimer in addition to that bound in situ.

If it is true that the self-association is induced by the binding of one vinblastine molecule per tubulin dimer, what is the role of the second vinblastine bound? As shown above, two alternatives are possible: either the second binding site is completely independent of the self-association or it is equivalent to the first one, so that the binding of one vinblastine molecule to any one of these two sites can induce the protein to self-associate. As shown in Table II, these two possibilities result in equally good linkages with identical protein association constants and ligand binding constants differing by a factor of 2. Comparison of the binding data of Lee et al. (1975) with the binding curves calculated from these two association mechanisms, shown in Figure 4A, favors mechanism 1b, i.e.,

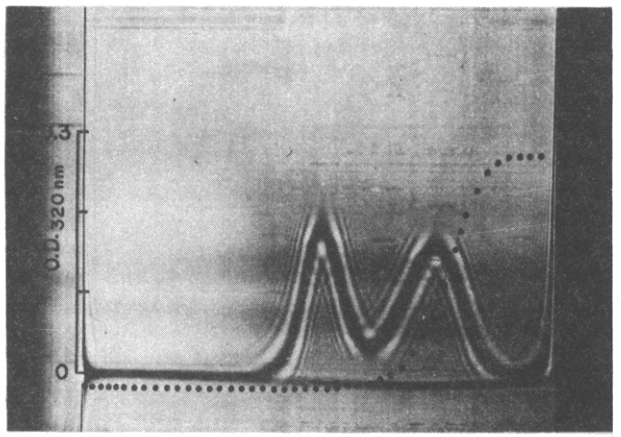

FIGURE 6: Bimodal sedimentation boundary of tubulin and vinblastine concentration distribution across the boundary. Tubulin was equilibrated with 1×10^{-5} M vinblastine–PG buffer. An aliquot from the equilibrating column, containing 16.6 mg/mL tubulin, was centrifuged at 60 000 rpm in a double-sector cell with the reference sector filled with 1×10^{-5} M vinblastine–PG buffer. The Schlieren picture was taken at a 65° bar angle 80 min after reaching speed. The dotted line depicts the photoelectric scan at 320 nm obtained simultaneously with the Schlieren picture.

two binding sites equally effective in inducing self-association, since the data were obtained at total protein concentrations above 2 mg/mL and the fit is best with the curves calculated for this mechanism at 2 and 4 mg/mL protein.

This mechanism was supported by one further piece of evidence, namely, the scanner tracings in the velocity sedimentation of tubulin in the presence of vinblastine. In these experiments, the vinblastine concentration distribution across the ultracentrifuge cell was determined by monitoring the solution absorption at 320 nm which arises exclusively from the vinblastine molecule. Tubulin was equilibrated with 1×10^{-5} M vinblastine in PG buffer and then centrifuged against the same vinblastine–PG buffer in the reference sector. The resulting Schlieren pattern and the optical absorption at 320 nm are shown in Figure 6. It is seen that in the supernatant region, which is depleted of protein, the solution absorbance at 320 nm is slightly lower than that of the equilibrating buffer, indicating that vinblastine has been depleted from the supernatant due to the differential transport of the tubulin monomers and polymers (Na & Timasheff, 1980). As sedimentation proceeds, the peak resolves into a bimodal pattern and the total vinblastine concentration in the region of the slow moving peak is essentially identical with that in the supernatant. Now, prior to the resolution of the boundary, the tubulin molecules in the slow moving peak were simply those which were unassociated in the equilibrium mixture of the original unresolved reaction boundary and which have lagged behind because of their slower sedimentation rate. Were the binding of vinblastine to one of the two sites independent of the self-association reaction, one would expect to observe some extra vinblastine bound to tubulin in the slow moving peak and hence a higher total absorbance at 320 nm for this region than that found in the supernatant solvent depleted of protein. These observations suggest, therefore, that the binding of one vinblastine molecule to any one of the two binding sites on each tubulin dimer can induce the protein to enter into the polymerization reaction and to sediment more rapidly. This argument is only qualitative. Its verification has been undertaken through a quantitative computer simulation study of ligand distribution across the bimodal sedimentation boundaries for the different reaction mechanisms, now in progress in our laboratory.

The vinblastine cross-linking mechanism of tubulin self-association was considered since it is consistent with several of the observations. First, it requires that each tubulin dimer should possess two vinblastine binding sites, while in the highly polymerized state the vinblastine/tubulin ratio should approach 1. This corresponds exactly to what is found in the vinblastine-induced tubulin paracrystalline aggregates (Bryan, 1972; Wilson et al., 1978). Further, the molecular structure of the vinblastine molecule itself is suggestive of this mechanism. Vinblastine is a dialkaloid composed of a vindoline and a catharanthine molecule, linked together by a single bond. It would seem quite possible, therefore, that the vindoline portion of the molecule could bind to the first site of one tubulin dimer, whereas the catharanthine portion of the molecule binds to the second site of another tubulin dimer, forming a cross-linking bridge. Such a mechanism is compatible with the observation of Ventilla et al. (1975) that the replacement of vinblastine with equimolar quantities of vindoline and catharanthine abolished the ability of the alkaloid to induce tubulin self-association. In spite of these favorable considerations, it is highly unlikely that the cross-linking mechanism is operative in this system, since the data cannot be fitted reasonably in terms of this mechanism as described by eq 15 and 16. The first disagreement is found in the comparison between the experimental and calculated linkages of the apparent association constant. As shown in Figure 3B, the experimentally determined apparent self-association constants increase continuously with increasing vinblastine concentration, while the same parameter calculated in terms of the cross-linking mechanism should reach a maximum at $[X] = 1/k_1$ and then decrease with a further increase in ligand concentration because of the competition of vinblastine for the available binding sites on the protein. As a result, ligand cross-linked macromolecules should approach the unassociated state at high concentrations of the ligand (Nichol & Winzor, 1976). This is contrary to observation. The second disagreement was found in the absolute value of the self-association constant. According to eq 16 and 17, the protein self-association constant in a cross-linking reaction should be either weaker than or of the same order of magnitude as that of the ligand binding constant. Our result that the apparent self-association constant is 1 order of magnitude higher than the ligand binding constant suggests further that the self-association of tubulin induced by vinblastine is not a simple cross-linking reaction by a divalent ligand, as had been found, for example, for the mercuric chloride induced association of mercaptalbumin (Edelhoch et al., 1953). It is worth mentioning here that Wilson et al. (1978) have shown that the sea urchin egg tubulin–vinblastine paracrystals did not dissociate on binding one vinblastine molecule per tubulin dimer in addition to the one found within the aggregates in situ, suggesting that these aggregates, as well, are not held together through simple vinblastine cross-links.

Finally, one should consider the discrepancy between the vinblastine binding constants reported from different laboratories (Lee et al., 1975; Wilson et al., 1975; Bhattacharyya & Wolff, 1976). A possible explanation may be found in the different experimental conditions used. The tubulins used had been isolated from different animals, using different purification procedures, and the vinblastine bindings were monitored by different techniques. One factor, however, which had not been considered in any of these studies is the self-association of tubulin in the presence of vinblastine and the necessary consequence that the binding constants observed are average values of binding to all protein species, both monomers and

polymers, in the solution. We have reexamined the vinblastine binding of calf brain tubulin in PG buffer previously reported from this laboratory (Lee et al., 1975) and have found these results to conform to the apparent vinblastine binding calculated when tubulin self-association is taken into account. In a similar examination of the vinblastine binding data reported by Wilson et al. (1975) and by Bhattacharyya & Wolff (1976), we noticed an important difference in the composition of the experimental media used. Namely, while Lee et al. (1975) had worked in PG buffer without any magnesium ions, the buffers used by Wilson et al. (1975) and Bhattacharyya & Wolff (1976) contained 5 and 10 mM Mg^{2+}, respectively. Magnesium ions, however, are known to enhance strongly the vinblastine-induced self-association of tubulin (Weisenberg & Timasheff, 1970). In our ultracentrifugation study, we noticed also that the protein, when equilibrated in PG–10 mM $MgCl_2$–5 × 10^{-5} M vinblastine, sedimented completely to the bottom of the cell before reaching 40 000 rpm, indicating that essentially all of the protein was in a highly aggregated form. More recently, Wilson et al. (1978) have found that the vinblastine-induced tubulin paracrystalline aggregates isolated from sea urchin eggs require the presence of Mg^{2+} ions in the buffer in order to prevent them from redissolving, pointing again to a cooperative role of Mg^{2+} in the vinblastine-induced aggregation of tubulin.

While the exact mechanism and thermodynamic parameters of tubulin self-association in the simultaneous presence of Mg^{2+} and vinblastine are unknown at present, we have calculated the effect of an enhanced self-association on the apparent binding constant of vinblastine, making the simple assumptions that (1) Mg^{2+} enhances the self-association constant of tubulin in the presence of vinblastine without affecting the vinblastine binding to tubulin dimers and that (2) the self-association induced by the binding of one vinblastine molecule per dimer still proceeds through an isodesmic, indefinite mechanism. The calculated binding curves with $k_1 = 1.8 \times 10^4$ M^{-1} and increasing k_2 are depicted in Figure 7. It is striking that the obtained Scatchard plots have the typical appearance of those normally attributed to two sites with different binding constants. Comparison of these curves with the tubulin–vinblastine binding data of Wilson et al. (1975) and of Bhattacharyya & Wolff (1976), plotted on the same figure, shows some similarities between the calculated binding curves and the experimental ones. In the calculated binding curves, although we have assumed that the two vinblastine binding sites per tubulin dimer have identical binding constants of 1.8×10^4 M^{-1}, the apparent binding for the first site appears to be much stronger, reflecting the linkage between the binding of the first vinblastine to the self-association. On the other hand, binding of vinblastine to the second site is not affected by the self-association in our model, and it manifests itself as an apparently weaker site in the calculated Scatchard plots. In this manner, apparent binding constants for the first site of the order of 10^6 and 10^5 M^{-1} can be obtained by choosing intrinsic self-association constants equal to 5.3×10^7 and 1.4×10^7 M^{-1}, respectively. It seems, therefore, that the magnitude of the apparent binding constants reported by the three laboratories correlates well with the Mg^{2+} concentrations used in the individual studies. Some differences do exist between the calculated and the experimental bindings. For example, the vinblastine binding data of Wilson et al. (1975) fall on a straight line in their Scatchard plot, whereas the best-fitted calculated binding isotherm is curved. This could be due either to uncertainty in the experimental data or to imperfections in the reaction mechanism assumed in our calculation. What

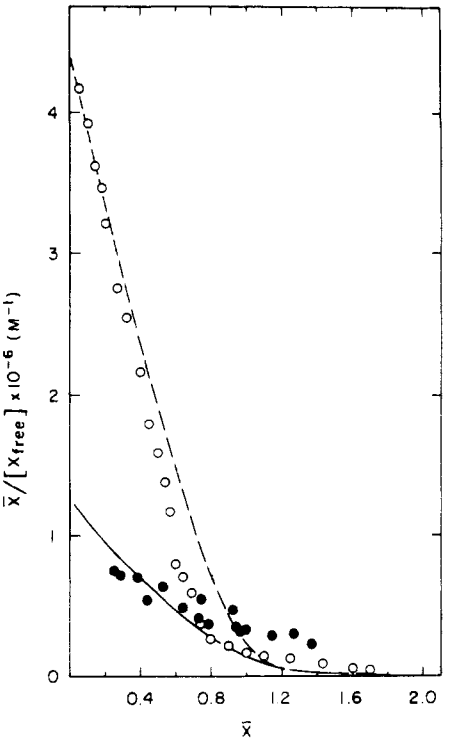

FIGURE 7: Comparison of theoretical ligand bindings calculated for a ligand-induced self-associating system with literature data on the binding of vinblastine to tubulin. The curves were calculated with the linkage equation for mechanism 1a of Table II by using $k_1 = 1.8 \times 10^4$ M^{-1} for both ligand binding sites and different values of k_2: (—) 1.4×10^7 and (---) 5.3×10^7 M^{-1}. Total protein concentration was 1 mg/mL. For a more detailed description of the mechanism and calculation, see the text. The literature data on the binding of vinblastine to tubulin are from (●) Wilson et al. (1975) and (○) Bhattacharyya & Wolff (1976).

is certain at this point, however, is that Mg^{2+} ions do enhance strongly the vinblastine-induced tubulin self-association, and apparent binding constants obtained through standard plots must necessarily appear to be higher than the intrinsic binding constant of ligand to monomer. Therefore, extreme caution must be exerted in correlating apparent binding constants with phenomena dependent on the binding, such as the inhibition of microtubule assembly and the induction of tubulin self-association. Noticing that tubulin self-association becomes prominent at 10^{-4} M vinblastine, i.e., at a molarity identical with the apparent dissociation constant of the weak binding site, Bhattacharyya & Wolff (1976) have proposed that the self-association of tubulin is induced by the binding of vinblastine to this weak binding site. However, the buffer which they had used in the binding and the self-association studies contained 10 and 0.5 mM $MgCl_2$, respectively. Had they used 10 mM Mg^{2+} throughout, they should have detected the aggregation of tubulin at a much lower concentration of vinblastine. Their second suggestion that the inhibition of microtubule assembly at vinblastine concentrations of 10^{-6} M is caused by the binding of vinblastine to the "high-affinity" site is probably also fortuitous. As pointed out by Wilson et al. (1975), in vitro microtubule assembly can be inhibited by substoichiometric amounts of vinblastine through a poisoning mechanism. This has been confirmed by Himes et al. (1976) and observed in our laboratory (G. C. Na & S. N. Timasheff, unpublished experiments). Consequently, both on thermodynamic and experimental grounds it becomes meaningless to make simple correlations between the apparent binding site dissociation constant and the free vinblastine concentration needed to inhibit in vitro microtubule assembly.

The inhibition of microtubule assembly at a vinblastine concentration of 10^{-6} M can be easily reconciled with an intrinsic ligand dissociation constant of 5×10^{-5} M, if one remains cognizant of magnitudes that free energy linkages may assume. Thus, while the affinity of vinblastine toward the two binding sites is weak, it can be greatly enhanced by a favorable standard free energy change in the linked macromolecular self-association reaction. In other words, were the assembling end of a microtubule to have a stronger affinity toward a vinblastine-liganded tubulin dimer than to a free one, the standard free energy available for holding the vinblastine at the growing end of a microtubule would be much more negative than that normally available for binding the ligand to free tubulin dimers. As a result, inhibition of microtubule growth could be complete at ligand concentrations much below the dissociation constant of vinblastine from tubulin dimers. This analysis makes it possible to understand thermodynamically the "poisoning mechanism" of the vinblastine inhibition of microtubule assembly, proposed by Wilson et al. (1975, 1976), if one makes only one further assumption. Namely, the insertion of a vinblastine-liganded tubulin dimer at the growing end of a microtubule must inhibit the addition of further tubulin dimers in the proper geometric order. It is quite evident, then, that inhibition of microtubule assembly by vinblastine at a concentration below 10^{-6} M and at a total amount substoichiometric to tubulin is fully permitted thermodynamically, even though the intrinsic binding constant of vinblastine to a tubulin dimer is only of the order of 10^4 M^{-1}. The existence of such a complex linkage is currently under scrutiny in our laboratory.

References

Aune, K. C., & Timasheff, S. N. (1971) *Biochemistry 10*, 1609–1617.

Bhattacharyya, B., & Wolff, J. (1976) *Proc. Natl. Acad. Sci. U.S.A. 73*, 2375–2378.

Bryan, J. (1972) *Biochemistry 11*, 2611–2616.

Cann, J. R., & Hinman, N. D. (1976) *Biochemistry 15*, 4614–4622.

Edelhoch, H., Katchalski, E., Maybury, R. H., Hughes, W. L., Jr., & Edsall, J. T. (1953) *J. Am. Chem. Soc. 75*, 5058–5072.

Himes, R. H., Kersey, R. N., Heller-Bettinger, I., & Samson, F. E. (1976) *Cancer Res. 36*, 2798–2802.

Inoue, H., & Timasheff, S. N. (1972) *Biopolymers 11*, 737–743.

Kegeles, G., & Cann, J. R. (1978) *Methods Enzymol. 48*, 248–270.

Klotz, I. M. (1953) *Proteins 1B*, 727–806.

Lee, J. C., & Timasheff, S. N. (1977) *Biochemistry 16*, 1754–1764.

Lee, J. C., Harrison, D., & Timasheff, S. N. (1975) *J. Biol. Chem. 250*, 9276–9282.

Na, C., & Timasheff, S. N. (1979) *Fed. Proc., Fed. Am. Soc. Exp. Biol. 38*, 796.

Na, G. C., & Timasheff, S. N. (1980) *Biochemistry* (preceding paper in this issue).

Nichol, L. W., & Winzor, D. J. (1976) *Biochemistry 15*, 3015–3019.

Owellen, R. J., Owens, A. H., Jr., & Donigian, D. W. (1972) *Biochem. Biophys. Res. Commun. 47*, 685–691.

Owellen, R. J., Donigian, D. W., Hartke, C. A., Dickerson, R. M., & Kuhar, M. J. (1974) *Cancer Res. 34*, 3180–3186.

Scatchard, G. (1949) *Ann. N.Y. Acad. Sci. 51*, 660–672.

Tai, M., & Kegeles, G. (1975) *Biophys. Chem. 3*, 307–315.

Tanford, C. (1969) *J. Mol. Biol. 39*, 539–544.

Timasheff, S. N. (1973) *Protides Biol. Fluids, Proc. Colloq. 20*, 511–519.

Ventilla, M., Cantor, C. R., & Shelanski, M. L. (1975) *Arch. Biochem. Biophys. 171*, 154–162.

Weisenberg, R. C., & Timasheff, S. N. (1970) *Biochemistry 9*, 4110–4116.

Wilson, L., Creswell, K. M., & Chin, D. (1975) *Biochemistry 14*, 5586–5592.

Wilson, L., Anderson, K., & Chin, D. (1976) *Cold Spring Harbor Conf. Cell Proliferation 3*, 1051–1064.

Wilson, L., Morse, A. N. C., & Bryan, J. (1978) *J. Mol. Biol. 121*, 255–268.

Wyman, J. (1964) *Adv. Protein Chem. 19*, 224–285.